

Article

Ecosystem Variability along the Estuarine Salinity Gradient: A Case Study of Hooghly River Estuary, West Bengal, India

Diwakar Prakash ¹, Chandra Bhushan Tiwary ²  and Ram Kumar ^{1,*} 

¹ Ecosystem Ecology Research Unit, Department of Environmental Science, School of Earth, Biological and Environmental Sciences, Central University of South Bihar, SH-7, Gaya-Panchanpur Rd, Fatehpur, Gaya 824326, Bihar, India

² Department of Zoology, Vidya Bhavan Mahila Mahavidyalay, Siwan 841226, Bihar, India

* Correspondence: ramkumar@cub.ac.in

Abstract: Hooghly River, a ~460 km long distributary of the Ganga River, passes through a highly industrialized Metropolis-Kolkata in West Bengal, India, and eventually empties into the Bay of Bengal at Gangasagar. To determine the patterns and drivers of planktonic community, spatiotemporal variations in water quality and micronutrient content and planktic prokaryotic and microeukaryotic abundance and diversity across the salinity gradient (0.1 to 24.6 PSU) in the Hooghly River estuary (HRE) were studied. Plankton and water samples were collected at six sites during October 2017, February 2018, and June 2018. The biotic parameters—phytoplankton (Chlorophyll *a*), total bacterial abundance (cfu), and copepods—were significantly higher in the downstream estuarine sites than in the upstream riparian sites; conversely, rotifer and cladoceran abundances were significantly higher at upstream stations. The most culturable bacterial strains were isolated from the two freshwater sites and one at the confluence (estuarine) and are characterized as *Bacillus subtilis*, *Pseudomonas songnenensis*, and *Exiguobacterium aurantiacum*. Among zooplankton, rotifers (0.09 ± 0.14 ind L⁻¹) and cladocerans (5.4 ± 8.87 ind L⁻¹) were recorded in higher abundance and negatively correlated with bacterial concentrations at upstream stations. On the temporal scale, February samples recorded lower proportions of bacterivorous zooplankton at the three upstream stations. Cluster analysis separated samples on the basis of seasons and water mass movement. The February samples showed distinct spatial characteristics, as three freshwater (FW) stations grouped together and segregated at second 2nd hierarchical level, whereas the three estuarine stations formed a separate cluster at the 50% similarity level. Samples collected in October 2017 and June 2018 exhibited mixed attributes. June samples recorded higher influence of freshwater discharge. The zooplankton abundance showed significant negative correlation with Chl *a*. Our results demonstrate the relative role of river continuum, land-driven lateral discharge, and seawater intrusion in shaping community structure, which needs to be considered in management and conservation planning of aquatic ecosystems, especially in highly productive and overexploited HRE.

Keywords: bacteria; estuary; river; plankton; trophic structure



Citation: Prakash, D.; Tiwary, C.B.; Kumar, R. Ecosystem Variability along the Estuarine Salinity Gradient: A Case Study of Hooghly River Estuary, West Bengal, India. *J. Mar. Sci. Eng.* **2023**, *11*, 88. <https://doi.org/10.3390/jmse11010088>

Academic Editors: Marco Uttieri, Ylenia Carotenuto, Iole Di Capua and Vittoria Roncalli

Received: 24 November 2022

Revised: 20 December 2022

Accepted: 26 December 2022

Published: 3 January 2023



Copyright: © 2023 by the authors. Licensee MDPI, Basel, Switzerland. This article is an open access article distributed under the terms and conditions of the Creative Commons Attribution (CC BY) license (<https://creativecommons.org/licenses/by/4.0/>).

1. Introduction

Estuaries are highly productive and dynamic semi-enclosed waterbodies linked to the sea either permanently or periodically and fed by freshwater from river inputs, resulting in a distinct salinity gradient and characteristics biota [1–5]. The complexity in a river estuary is determined by the variability in river water mixing with sea water, resulting in salinity [6], turbidity, and nutrient gradients [7–10]. There has been a long debate about the functioning of estuaries [11–13]; the community structure of phytoplankton, bacterioplankton, and zooplankton; and their relationship and their co-occurrence pattern [14,15]. The common consensus is that planktic communities play a key role in maintaining the ecological functioning of an estuary [16].

The Hooghly River is one of the most important estuarine systems in India because of the discharge from a vast river basin with substantial monsoonal precipitation ($70,500 \text{ m}^3 \cdot \text{s}^{-1}$ peak flow at Farakka), its origin from the largest montane river (~2600 km), and its long tidal zone (~280 km). Being an active tidal estuary, it has distinct biological and physico-chemical characteristics [17]. The commissioning of Farakka Barrage in 1975 facilitated the adequate quantity of Ganga water in the Bhagirathi-Hooghly River system, improving the ecosystem health and riverine-estuarine biodiversity [18–21], finally manifesting as seaward pushing the salinity zone in the estuary [22]. Fish species such as *Rita rita*, *Sperata seenghala*, *Eutropiichthys vacha*, *Wallago attu*, *Clupisoma garua*, *Labeo calbasu*, and *Catla catla* have made their emergence in the upper zone of the Hooghly River estuary (HRE), namely Tribeni and Banlagarh [23], which were reported from this zone before 1975, i.e., prior to the commissioning of the barrage. HRE provides valuable a nursery and recruitment habitat for commercially important species, such as Hilsa, finfish, and shrimp [24,25].

Any short-term or long-term changes are immediately reflected by the change in planktonic community [26,27], as they are self-sustaining, constituting the important components of the microbial loop while channeling carbon and energy from microbes to higher trophic levels by joining the classical food web [14,28–30] in aquatic ecosystems. The microbial loop explains pathway of carbon flow through nutritional food web that begins with dissolved organic matter (DOM) and reaches to the highest trophic levels bypassing some and passing through various trophic levels. The main stakeholders of the microbial loop include bacteria, zooplankton, phytoplankton, and other nutrient-cycling organisms [14,30,31]. The relative densities of bacterivorous, herbivorous, carnivorous, and omnivorous zooplankton are a reliable indicator of the functioning of the microbial loop and of ecosystem health on the spatial scale [32,33]. The zooplankton community comprises diverse feeding groups, such as bacterivores, detritivores, herbivores, and carnivores [34–36], forming a bridge between the microbial loop and classical food web. Information concerning co-occurrence, distribution, and community composition of the prokaryotic and eukaryotic plankton in the HRE is lacking [37,38]. The spatiotemporal variations of planktonic communities are highly affected by the hydrochemical parameters and physical forces [26,27,39–41]. Therefore, major components of microbial loop, i.e., bacterioplankton, phytoplankton and zooplankton, are likely to be affected by these activities. However, their co-occurrence and distributional patterns have not been studied in the HRE at a spatial scale ranging from fresh water to the estuary mouth. The knowledge of bacterioplankton–zooplankton co-occurrence is very essential, as zooplankton might act as a biotic selector for a specific microbial loop [42]. Bacterioplankton in the present study include culturable strains only because isolation of microbes is still necessary for the extraction of bioactive compounds [43], and this is accomplished by culture-based technique. Descriptions of new taxa of prokaryotes and experimental validation of microbial, ecological, and evolutionary processes are reliably based on culture based techniques. Therefore, this study isolated culturable bacterial strains and concentrated on culture-based methods.

The present study aims to elucidate the heterogeneity and co-occurrence of planktonic community along the salinity gradient ranging from freshwater to the estuary mouth and ecological drivers shaping the planktonic community structure in the HRE. To achieve these objectives, the study identified the ubiquitous nature and heterogeneity in distribution patterns of aquatic biological communities, including bacterioplankton, phytoplankton, and zooplankton (Rotifera, Cladocera, and Copepoda), at spatial scales during October 2017, February 2018, and June 2018 in the HRE, India. The samples were collected at six sites along the main salinity axis (0.1 to 25 PSU), from Barrackpore before the metropolis Kolkata to the estuary mouth. To elicit whether the co-occurrence or abiotic parameters are responsible for differential distribution patterns, we estimated water quality and micronutrient concentrations at all the six sites. At stations where higher correlation coefficient values for Bacteria *vs.* Rotifera abundance ($R = -0.76$) were recorded, we isolated the bacterial strain with >50% occurrence for further characterization.

2. Materials and Methods

2.1. Study Site

The HRE is a part of Ganga River system that originates from Bhagirathi (upper stretch), flows southwards through the lower Ganga deltaic plane, and merges with the Bay of Bengal in Sundarbans as the Hooghly River in West Bengal, India (Figure 1). Kolkata city, one of the largest metropolises along the Hooghly River, having a population of about 14.5 million, utilizes the river water for drinking and domestic and industrial purposes and also discharges sewage and sludge into the river [44]. Beginning upstream of the metropolitan city of Kolkata and downstream to the confluence, six sampling sites were chosen comprising the agricultural-industrial-anthropogenic and riverine (salinity: 0.1 to 0.45 PSU)-estuarine (salinity: 4.32 to 24.6 PSU) salinity gradient along the HRE (Figure 1).

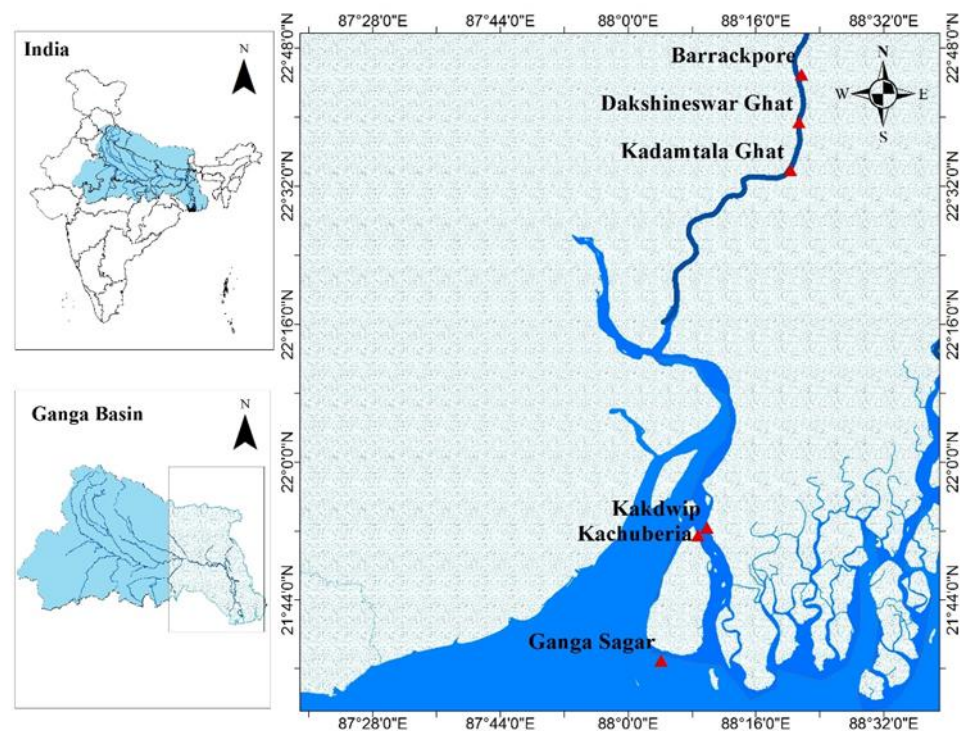


Figure 1. Geographic distribution of sampling sites along the Hooghly River estuary. Red triangles indicate the location of six sampling stations from Barrackpore to the confluence at Gangasagar (Bay of Bengal).

Sampling of surface water was performed at three riverine and three estuarine sites during the post-monsoon season, i.e., October 2017 and spring–February 2018, the and pre-monsoon season, i.e., June 2018, in the HRE (Figure 1). Samples were collected in cleaned polypropylene bottles from the surface to 20 cm depth for physio-chemical, bacteriological, phytoplankton, and zooplankton analysis. The details of sampling sites, abbreviations used hereafter, and common stressors at each site are provided in Table 1.

2.2. Environmental Parameters

In total, we collected 72 surface water samples in pre-cleaned, acid-washed polythene bottles for water quality analyses during the three sampling cruises. The salinity was determined by Hanna Instruments HI98319 marine salinity tester, as salinity has influence on the demography of zooplankton [45]. For the determination of dissolved oxygen, the Winkler titration method was used. Surface water temperature was measured using a mercury glass thermometer. The flow rate was measured by mechanical flow meter (hydrobios model 438110) The dissolved nutrients (nitrate and phosphate) were estimated by colorimetric methods (following [46]) using a spectrophotometer (PerkinElmer UV/VIS Spectrometer Lambda 25, Waltham, MA, USA) after filtering the water through 0.45 μm

filter paper (GF/F-Whatman, Maidstone, UK) within 12 h of sampling, and the filtered waters were stored in 100 mL pre-cleaned, acid-washed polythene bottles at 4 °C. All the parameters were analyzed following the standard procedures for water sampling and examination of water quality [47].

Table 1. Ecological stressors, abbreviations used, and coordinates of the six stations in the HRE sampled during October 2017, February 2018, and June 2018 for the present study.

Sampling Stations (Code)	Coordinates	Altitude (ft) ASL	Salinity (PSU) Trophic Status N:P Ratio	Ecological Stresses
Barrackpore (BRK)	22.75272° N 88.36212° E (Gandhighat)	13.12	0.1–0.42 13:0.04	Industrial effluents, domestic sewage disposal, boating, bathing, occasional Immersion of idols
Dakshineswar (DKS)	22.65643° N 88.35682° E (Dakshineshwarghat)	9.8	0.14–0.45 (18:0.092)	This site is 128 km away from the sea mouth of the river and has an estuarine condition due to significant tidal oscillation of ~3 m. Here, the river flows through the densely populated region in Kolkata city. Mostly untreated sewage disposes into river water near Dakshineswar ghat. The river water is also accessed for washing, bathing, and for many religious rituals
Kadamtala (KDM)	22.565° N 88.3387° E (Kadamtalaghat)	3.2	0.13–0.45 (14:0.052)	Bathing, Washing clothes, domestic effluents, ferry service, spiritual rituals, immersion of idols, oil leaching, leakage of oil from mechanized boat.
Kakdwip (KDP)	21.87208° N 88.16383° E (Harwood Point Ferry service)	0	4.32–10.64 (43:0.10)	Frequent dredging, boating, fishing, etc.
Kachuberia (KCB)	21.85903° N 88.14433° E (Kachuberiaghat Near govt. Jetty Gangasagar)	0	6.29–17.79 (60:0.18)	Frequent dredging, boating, fishing, etc.
Gangasagar (GS)	21.63307° N 88.07498° E (Gangasagar Mohana sea Beach)	0	13.09–24.6 (74:0.33)	Boating, tourist activities, dredging, fishing

2.3. Bacteriological Analysis

2.3.1. Enumeration, Isolation, and Characterization of Culturable Bacterial Strains

To study the bioactive potential for further prospecting, we estimated culturable bacterial concentrations and isolated the most culturable strains from three different sites. Five replicates of the water samples were collected in sterile polypropylene bottles from the surface to 15–20 cm deep and transported to the laboratory at 4 °C in an icebox (Table 1; Figure 1) during October 2017, February 2018, and June 2018. In the laboratory, water samples were stored at –21 °C until further processing. In the laboratory, bacterial concentrations were estimated by direct plate count method following [48]. The surface water samples, collected from different sites along an anthropic gradient in the HRE, were spread on media plates. Total bacterial density (colony forming unit: CFU mL⁻¹) was enumerated on nutrient agar plate, which was incubated at 37 °C for 24 ± 1.5 h [48]. The bacterial counts obtained were used to estimate the number of bacteria grown on the media plates used for DNA extraction. Colonies with different morphologies were subcultured into pure cultures by inoculating them into freshly prepared agar plates [49]. The most

abundant colony at each of the three sites was recorded for subsequent identification and statistics. At two sites, BRK and DKS were recorded for relatively higher abundance of bacterivorous zooplankton and higher strength of association between bacterioplankton and zooplankton. With an aim to identify highly abundant bacterial colony at these three sites (BRK, DKS, and GS), we isolated the bacterial colony with 50–70% occurrence and further cultured for sequencing and phylogenetic analysis [48,50].

2.3.2. Clustering, Alignment, and Phylogenetic Analysis of 16S rRNA Gene Fragments in Most Culturable BRK2, DKS, and GS1 Bacterial Strains

DNA from the bacterial culture—BRK2, DKS, and GS1 strains—was isolated using the bacterial gDNA isolation kit (XcelGen, Gujarat, India). Isolation of DNA was carried out according to manufacturer's instructions. First, 1.2% agarose gel was used to evaluate the quality of isolated DNA, and a single band of high-molecular band of the PCR amplicon was detected (Figure S1). Amplification of isolated DNA was performed with 16S rRNA-specific primer (8F and 1492R) using Veriti® 96 well thermal cycler (Model No. 9902, Thermo Fisher Scientific, Waltham, MA, USA). Sanger sequencing was performed using BDT v3.1 Cycle sequencing kit with M13F and M13R primers on ABI 3730xl Genetic Analyzer was performed after the PCR amplicon was enzymatically purified. A consensus sequence of 1284, 1465 bp, and 1487 of 16S rRNA was generated by using aligner software from forward- and reverse-sequence data. The consensus sequence of all the three strains, accession numbers, and origin are shown as Table S1. All nucleotide sequences were deposited at the National Center for Biotechnology Information (NCBI) strain library with accession numbers provided in (Table S1).

The evolutionary history was inferred by using the maximum likelihood method and Tamura–Nei model [51]. The tree with the highest log likelihood (−10,338.41, −10,518.13, −10,395.19) is shown, respectively, for BRK, DKS, and GS strain. Initial tree(s) for the heuristic search were obtained automatically by applying neighbor-joining and BioNJ algorithms to a matrix of pairwise distances estimated using the Tamura–Nei model and then selecting the topology with superior log likelihood value. This analysis involved 61 nucleotide sequences. There were a total of 1284, 1465, and 1484 positions in the final dataset of each strain (BRK, DKS, and GS). Evolutionary analyses were conducted in MEGA11 [52].

2.4. Phytoplankton Analysis

For qualitative analyses, five replicates of 1 L surface water samples were preserved in neutral Lugol's solution (1% Lugol's solution and 4% formalin) and brought to the laboratory for species identification. In the laboratory, samples were concentrated 10 times by centrifugation, and algal cells were observed on a Sedgewick rafter cell under a compound microscope (10×–400× magnification), and abundant species were identified using the standard key [53–57] and AlgaeBase (www.algaebase.org (accessed on 12 July 2018)) [56]. The amount of primary productivity was estimated in terms of chlorophyll *a* (Chl *a*). Chlorophyll pigment was analyzed through extraction using a mixture of dimethyl sulfoxide and 90% acetone [58] and enumerated by spectrometry using a Turner TD-700 fluorimeter (New York, NY, USA) following the standard method [46,59].

2.5. Zooplankton Analyses

Zooplankton samples were collected by making surface tows (0–20 cm) with a customized plankton net with 53 µm mesh size, 0.25 m mouth diameter, and preserved in 4% (*w/v*) buffered formalin immediately after collection in a 100 mL transparent bottle. At each site, 100 L water was filtered in five replicates. In the laboratory, the plastic bottles containing preserved zooplankton were thoroughly mixed, and a 1 mL subsample was drawn with a fine pipette to a Sedgewick–Rafter plankton counting cell for enumeration under the compound microscope (model no: Olympus CX21LED, Bartlett, TN, USA). The

numbers per liter of each genus was quantified and calculated using the following formula:

$$N = \frac{A \times C}{L}$$

where N denotes the number of plankton per liter, A is the average number of plankton in all counts, C is the volume of original concentrate in ml, and L is the volume of original water filtered, expressed in liters. Zooplankton species were identified to their lowest possible taxon [60–66].

Trophic-Based Zooplankton Community Analysis

Based on the published literature (Supplementary Table S5) and our own observations on propensity of feeding [35,67–71], the zooplankton communities identified at each station were characterized on the basis of functional feeding mode. Different fractions of zooplankton representing bacterivorous, herbivorous, carnivorous, and omnivorous types were segregated following standard literature [34–36,69,71–78] and analyzed separately.

2.6. Data Analysis

To elicit variations at spatio-temporal scales, the similarities of community composition among the sampling stations for each sampling date and also among sampling dates were compared. We first determined the centroid vector that represents the average composition of the group/species. Spatial heterogeneity was estimated using the mean and standard deviation of the similarities from the estimated similarity vector. We calculated the Bray–Curtis index to characterize the dissimilarities between samples (β -diversity). Square-root-transformed species abundance data were used for constructing the Bray–Curtis matrix of dissimilarity with average linkages group classification [79]. As the Bray–Curtis similarity mixes the differences due to species losses and species turnover, we also partitioned this index to understand both components of dissimilarity. For abiotic parameters, the distance between two samples was measured by Euclidean distance (ED), as ED is more appropriate for a low-dimensional data set [79].

To characterize the zooplankton diversity present in each sample (α -diversity), we calculated the Shannon diversity index (H') ($H' = -\sum(\text{Pi} \times \text{Log}(\text{Pi}))$) (Shannon, 1948), evenness index (J') ($J' = H' / \text{Log}(S)$) [80], and species richness (d) ($d = S - 1 / \text{Log}(N)$) [81]. To determine the variations among samples, non-metric multidimensional scaling (NMDS) ordination was computed based on Euclidean distance [82]. To identify the drivers of species abundance, pairwise correlation of water quality, and biotic parameters, the degree of a linear association between any two of the parameters was measured using Pearson's correlation coefficient (R). To test the distribution of data, the Shapiro–Wilk test of normality was used, and outliers were detected using scattering plot prior to Pearson's correlation analysis. Highly correlated parameters that may influence the community structure were identified. Indexes of dissimilarity, Shannon's index (α -diversity), Pielou's index (evenness), and Euclidean distance were calculated with PRIMER-version 6.0.

3. Results

3.1. Spatio-Temporal Patterns

All the estimated abiotic (Figure 2) and biotic (Figure 3) parameters except DO level, rotifer (Figure 3B), and cladoceran abundance, showed significant seaward increase; in contrast, the rotifer abundance showed a significantly seaward decreasing trend ($R^2 = 0.6$; $p < 0.0001$).

3.2. Physicochemical Parameters

The surface water temperature ranged from 26–29 °C with an average of 27 °C and recorded a significant ($R^2 = 0.3$; $p < 0.02$) seaward increase (Figure 2A). The highest average concentration of Ca^{++} , Na^+ , and K^+ was found at the mouth (Figure 2A–C; Table S2). The trophic level-related parameters (nitrate, phosphate, bacterial concentration, and Chl *a*) showed higher values in the estuarine stations (Table S2; Figure 2J,K); however,

the mean Chl *a* level was the highest at KCB station preceding the GS (Figure 3C). The dissolved oxygen concentration ranged from 6 to 8.2 mg·L⁻¹ but had disorderly spatial variation. The flow rate of the Hooghly River was recorded 0.3 m·s⁻¹ in February and 1 m·s⁻¹ in August.

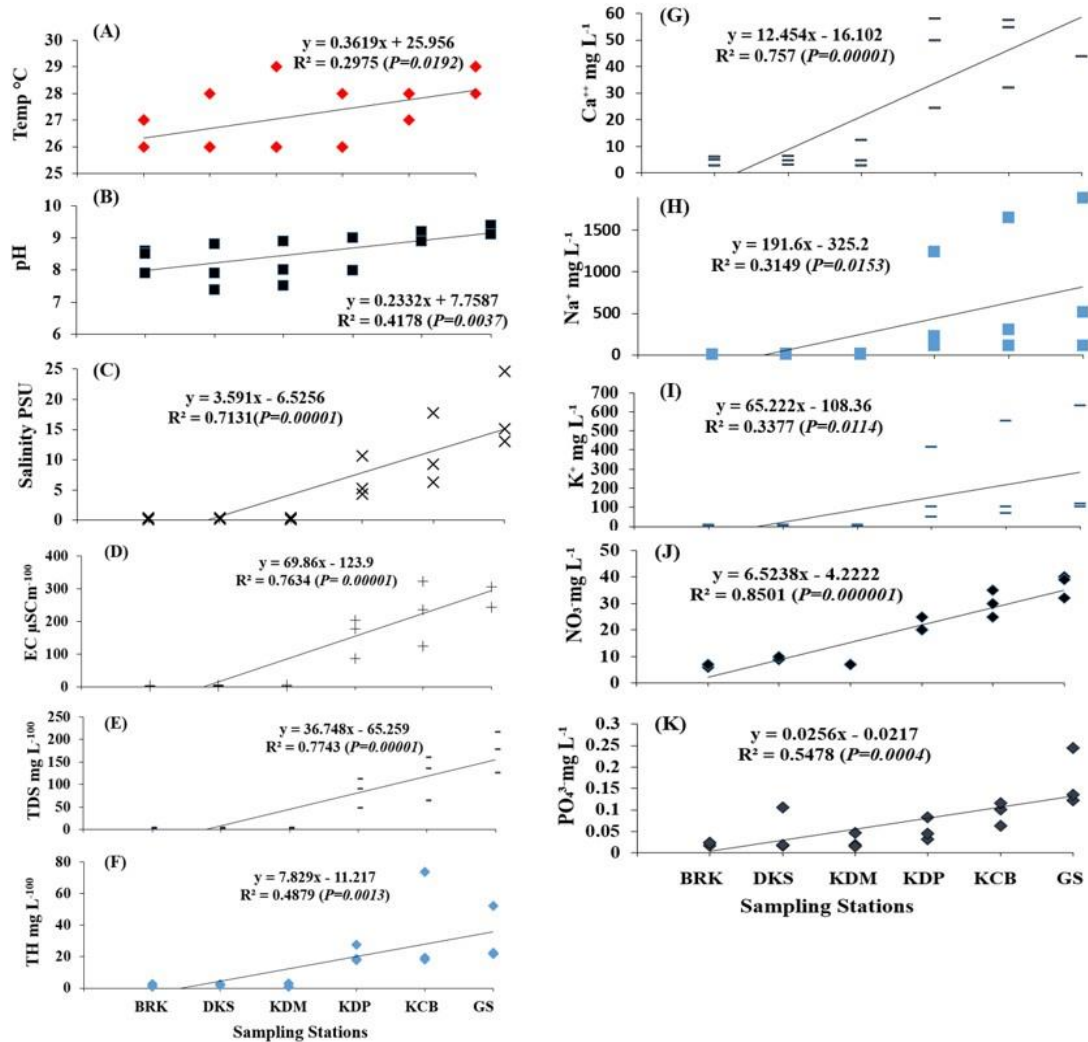


Figure 2. Seaward trends of selected physical parameters estimated for the present study at six sampling sites (Table 1) during October 2017, February 2018, and June 2018, including (A) temperature, (B) pH, (C) salinity, (D) electrical conductivity, (E) total dissolved solids, (F) total hardness, (G) calcium, (H) sodium, (I) potassium, (J) nitrate, and (K) phosphate.

3.3. Phytoplankton

The phytoplankton species recorded in the sampling stretch were *Pediastrum*, *Spirogyra*, *Coscinodiscus*, *Cyclotella*, *Melosira*, *Ankistrodesmus*, *Aulacoseira*, *Coelastrum*, *Microcystis*, *Oscillatoria*, *Anabaena*, *Aphanocapsa*, *Coscinodiscus radiatus*, *Pleurosigma formosum*, *Coscinodiscus lineatus*, *Biddulphia sinensis*, and *Chaetoceros lorenzianus* (Table S3). The mean Chl *a* concentration varied from 29.1 mg L⁻¹ to 219.9 mg L⁻¹, showing significant increase towards the river plume; the mean Chl *a* concentration was the highest at KCB station preceding the confluence GS (Figure 3C). The Chl *a* values showed positive correlation with all the abiotic parameters; however, a significant positive correlation was recorded with nitrate (R = 0.79) and Ca²⁺ ion concentration (R = 0.76). With biotic components, the significant negative correlation was recorded between Chl *a* values and zooplankton abundance (Table S6).

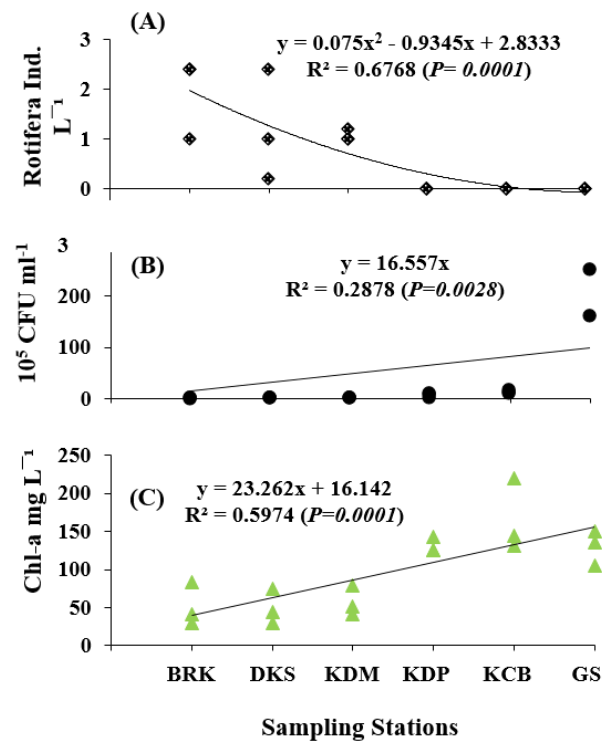


Figure 3. Seaward trends of selected biological parameters estimated for the present study at six sampling sites (Table 1) during October 2017, February 2018, and June 2018 including (A) Rotifera, (B) bacterial density, and (C) chlorophyll-*a*.

3.4. Zooplankton Community Structure

The symmetric map of all the parameters estimated, in rows and columns in principal coordinates, is given in Figure 4, in which the response category points to separate stations on an ordinal scale. Looking at the spatial scale with respect to the horizontal principal axis, all the zooplankton community at all the riverine stations aggregated together on the right side, whereas the last station at the confluence was set aside from other stations and positioned on the left, showing higher variation among sampling seasons (Figure 4).

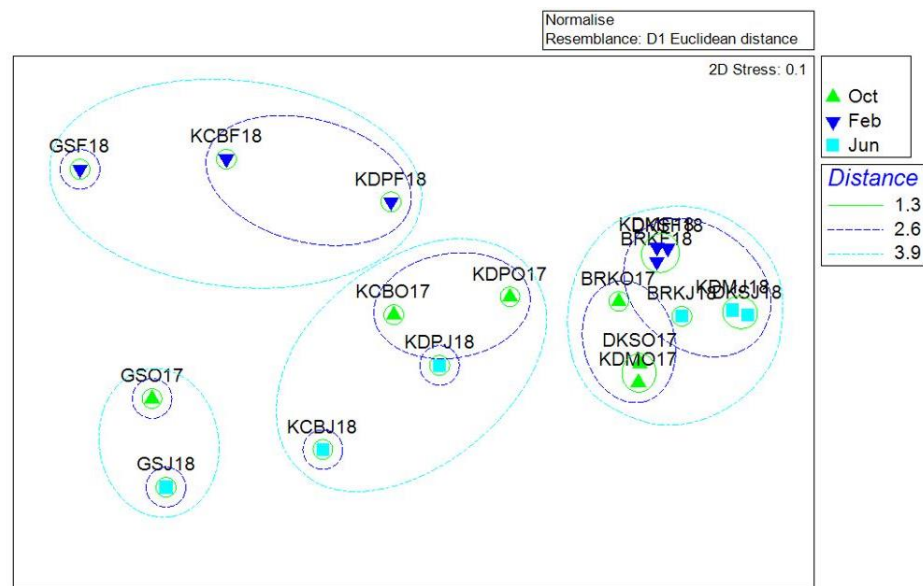


Figure 4. Non-metric multidimensional scaling (NMDS) of all the 18 samples collected from HRE, measured by the Euclidean distance.

The right extreme position of all the riverine samples and their unique position in the middle of the second (vertical) axis indicates that the responses are more in the intermediate categories of the scale rather than a mixture of extreme responses at the temporal scale (Figure 4). The scale values of these samples optimally discriminate between the 18 samples (6 stations \times 3 seasons), giving maximum between-sample variance. The second dimension then separates out samples on the basis of seasons, and all the estuarine samples collected in February are polarized towards the top. Upstream estuarine stations (KCB and KDP) aggregated inside, where both extremes of the response scale as well as the missing response are located (Figure 4). As a result, samples were arranged in the ordination of downstream confluence to freshwater stations from left to right. All KDP samples and KCB October samples are in a unique position inside, with relatively high polarization of responses and high missing values. Their position in the middle of both axes reveals more responses in the scale’s intermediate categories rather than a mixture of extreme responses at the spatiotemporal dimension. Figure 4 depicts the principal inertias at the positive ends of each axis, which were measured by adding together the percentages of inertia, i.e., $63.1\% + 13.3\% = 76.4\%$. This shows a “residual” of 23.6%, which is not shown in the map.

The unique right-side positioning of all the riverine stations may be attributed to the presence of rotifers (0.09 ± 0.14) and cladocerans (5.4 ± 8.87) in dL^{-1} , captured at upstream freshwater stations only, whereas copepods were present at all stations (Figure 5A). Integrating all zooplankton samples (Figure 5A; Table S4) were dominated by the Copepoda (92%) followed by Cladocera (7%) and Rotifera (1%). Total zooplankton abundance was more affected by seasons and showed a disorderly distribution among stations. Zooplankton density showed a peak in February (beginning of spring) at all sampling stations except KDM, where the peak was recorded in June samples (Figure 5A). The peak of the total zooplankton abundance was mainly contributed by the copepods at all stations (Figure 5A). At the three riverine stations, the rotifer densities were significantly lower during the peak of the total zooplankton abundance (Figure 5A). The indices of diversity, richness, and evenness of zooplankton recorded at six selected stations in the HRE are provided in (Figure 5B–D).

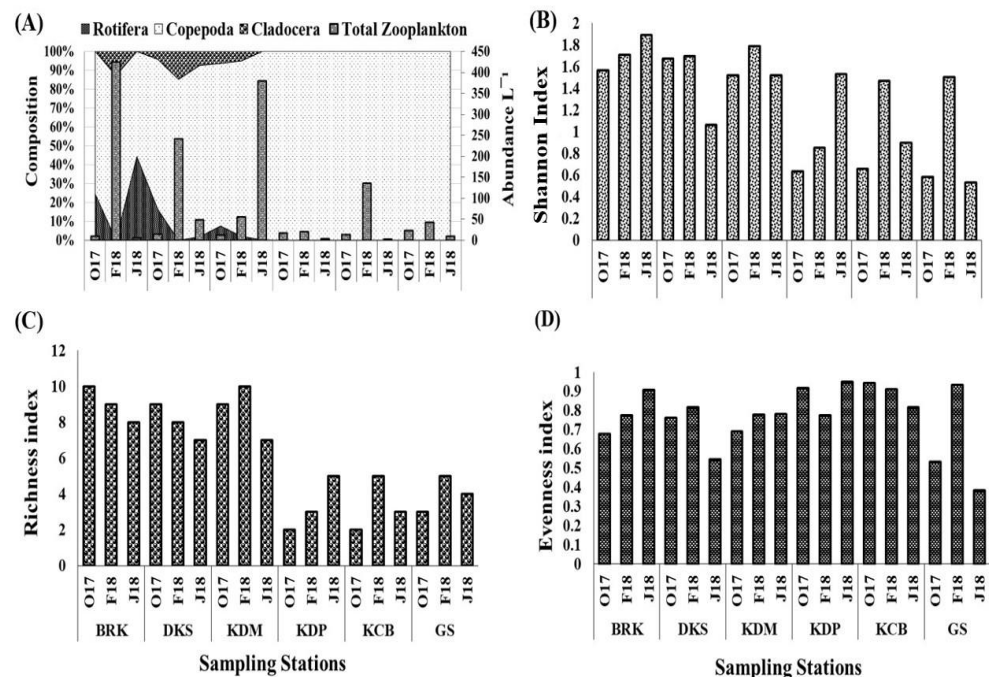


Figure 5. Percent (%) composition of Rotifera, Cladocera, Copepoda, and total zooplankton abundance (L^{-1}) (A), Shannon–Wiener index of diversity (B), species richness (C), and Simpson index for evenness (D) of zooplankton, recorded during October 2017, February 2018, and June 2018 at six selected stations in the HRE.

The heterogeneity at the spatial scale was estimated by the Bray–Curtis similarity matrix, which was observed to be higher than the heterogeneity at the temporal scale (Figure 6). It shows that the average similarity between all sampling dates was higher than the average similarity between the stations on a single sampling date. The cluster analysis gives further insights into the relative role of seawater and freshwater in shaping the community structure and segregate stations accordingly (Figure 6). The first hierarchical level separates the June samples of DKS and KDM and February samples of the two uppermost stations (BRK and DKS) from the remaining samples at 90% dissimilarity, from which June samples of DKS were separated at the second hierarchical level at 75% dissimilarity. June samples of DKS mainly represented the Cyclopoida adults, copepodites, and the Cladocera *Moina macrocopa*, whereas February samples of upper two stations and June samples of KDM grouped together and represented copepod nauplii, cyclopoids, and calanoids. The June samples of BRK, KDP, and KCB grouped together and separated at the third hierarchical level, whereas the February samples of all the estuarine and lowermost riverine (KDM) stations grouped together and separated at the fourth hierarchical level. Samples collected in February 2018 at the three estuarine stations and the lower most riverine (KDM) station grouped together and separated from remaining samples at the hierarchical level V (VIIB). The highly indicative zooplankton of cluster VIIB are copepod nauplii and harpacticoids (Figure 6). This cluster clearly indicates further upward intrusion of the marine community in February. All the October samples aggregated at intermediate position and showed clear separation of riverine and estuarine stations (Figure 6). October samples showed distinct spatial variations, where riverine samples were separated from estuarine samples at the fifth hierarchical level, and the June samples of GS (estuarine mouth) joined this cluster (Figure 6).

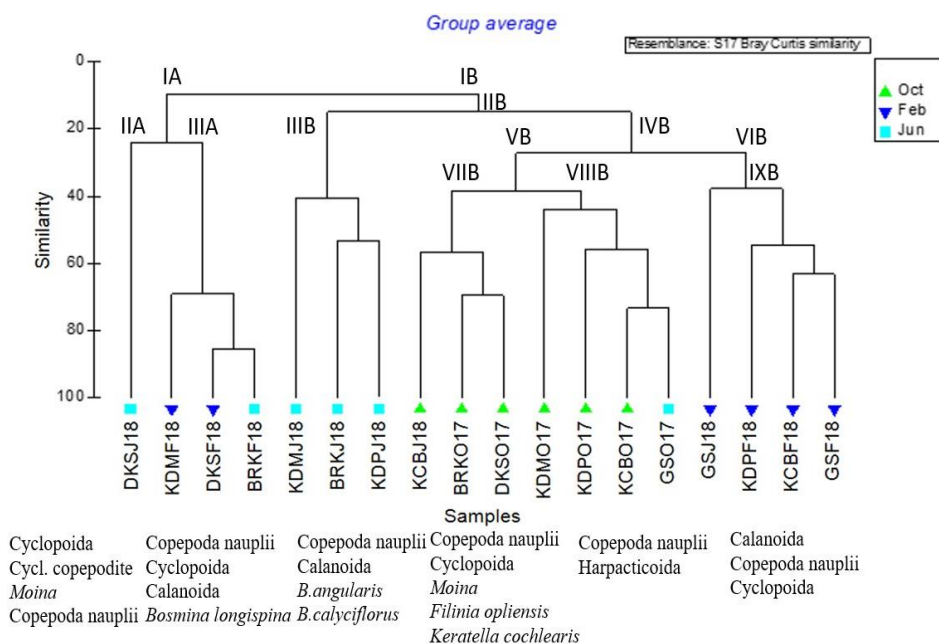


Figure 6. Bray–Curtis similarity of zooplankton and most abundant taxa for each cluster at six sampling stations during (October 2017, February 2018, and June 2018) in the HRE.

The trophic-based structuring of the zooplankton community revealed that the community was dominated by the omnivores followed by the herbivores and the bacterivores, respectively (Figure 7A–C). Variations in trophic-based community structure were more prominent at the spatial scale than the temporal scale. Bacterivorous and detritivorous species were recorded at upper stations and limited to KDP, whereas downstream stations mainly represented the omnivorous copepods (Figure 7A–C). Detritivores were mainly represented by the bdelloid rotifers at BRK and DKS. Differences in bacterivorous fraction of zooplankton community were not significant among the three riverine stations

(Figure 7A–C); however, at temporal scale, February samples recorded significantly lower fractions of bacterivorous zooplankton at all the three riverine stations.

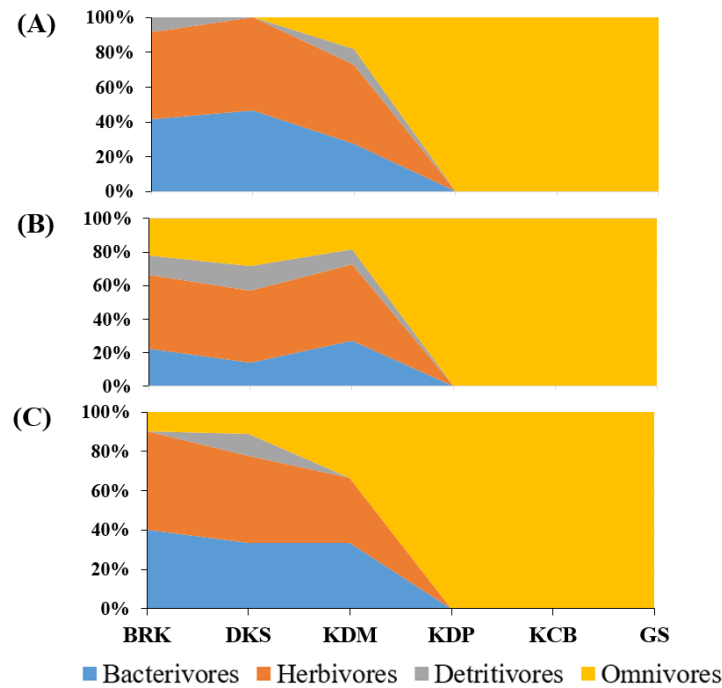


Figure 7. Percent (%) composition of zooplankton trophic guild at six sampling stations during October 2017 (A), February 2018 (B), and June 2018 (C) in the HRE.

3.5. Bacteriological Analyses

Total culturable bacterial density CFU mL^{-1} varied from 0.06 to $300 \times 10^5 \text{CFU mL}^{-1}$ at six selected sampling stations during October 2017, February 2018, and June 2018 in HRE. With the lowest bacterial concentration at Barrackpore and the highest at Gangasagar, unique spatial differences and significant seaward ($R = 0.66$ $p < 0.0028$) increase in density of culturable bacteria were recorded in the present study (Figure 8).

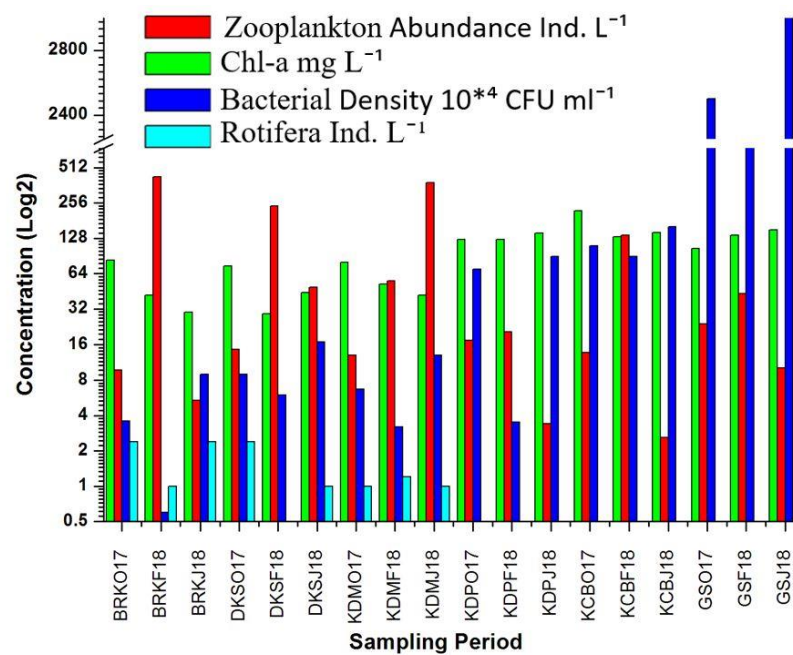


Figure 8. Total Rotifera (Ind L^{-1}), bacterial density (CFU mL^{-1}), total zooplankton abundance, and Chl *a* recorded in October 2017, February 2018, and June 2018 at six sampling stations in the HRE.

Overall bacterial densities were higher at downstream stations (KDP, KCB, and GS) than the upper freshwater stations (BRK, DKS, and KDM). Amongst upstream stations, bacterial densities were negatively correlated with total rotifer density and Chl *a* concentration; however, the correlation was significant for Bacteria *vs.* Rotifera abundance only (Figure 9; Table S6, $p < 0.01$). The most abundant culturable strains were *Bacillus subtilis*, *Pseudomonas songnensis*, and *Exiguobacterium aurantiacum*, respectively, at BRK, DKS, and GS (Figure 10).

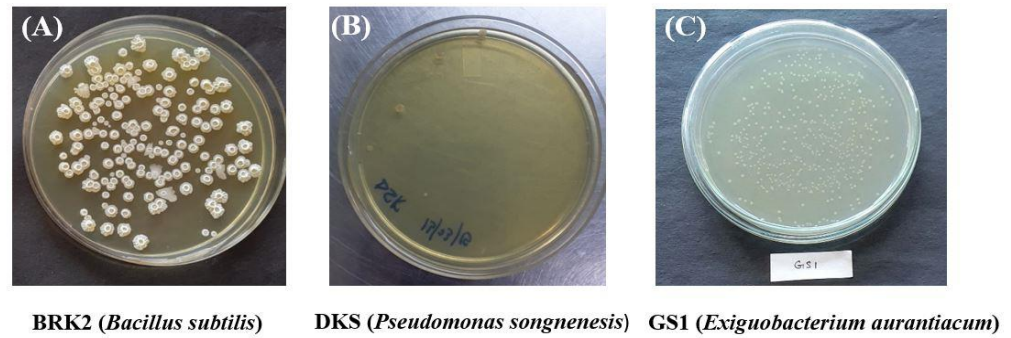


Figure 9. Most dominant bacterial strains *Bacillus subtilis* (A), *Pseudomonas songnensis* (B), and *Exiguobacterium aurantiacum* (C) isolated from three selected sampling stations (BRK, DKS, and GS) in the HRE.

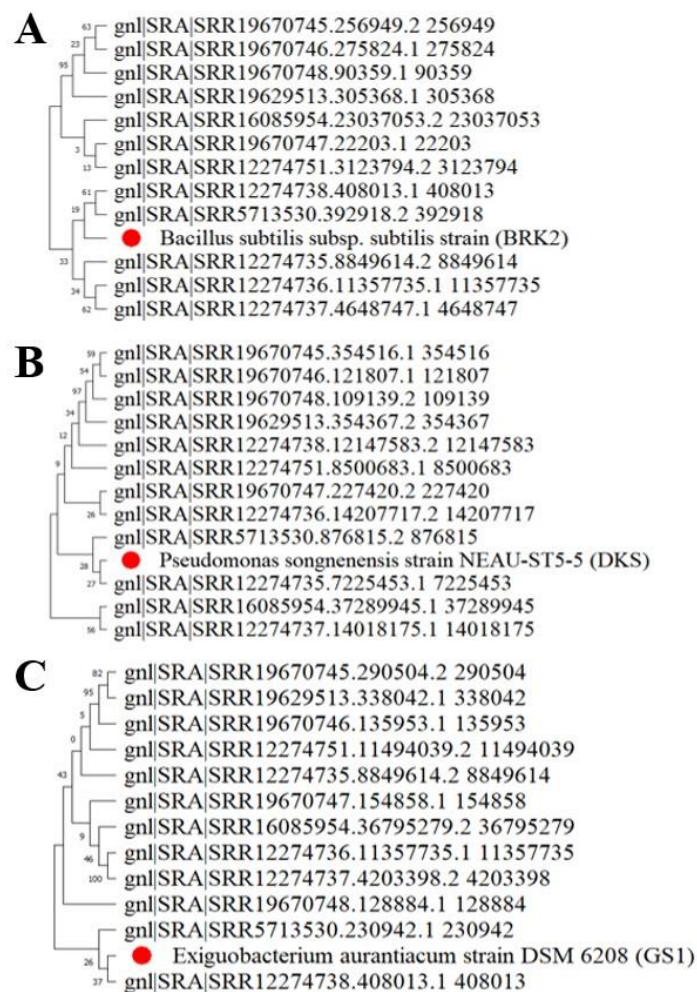


Figure 10. Phylogenetic analysis of *Bacillus subtilis* (A), *Pseudomonas songnensis* (B), and *Exiguobacterium aurantiacum* (C) with their twelve different orthologues, isolated from three selected sampling stations (BRK, DKS, and GS) in the HRE.

3.6. Characterization of Highly Abundant Bacterial Taxa at BRK, DKS, and GS

The branch lengths and topology of a phylogenetic tree of the isolated strains were attained by the maximum likelihood technique. The phylogenetic trees were formed based on evolutionary distance data of 16S rRNA gene sequences. The tree shows the integrated relationship of the isolated strains with most similar Gangetic bacterial species genes based on highly similarity 95–100% taken from the 12 different Gangetic samples generated by illumine and Nanopore sequencing platforms Figure 10A–C.

3.7. Interrelationship among Taxa

The pairwise multiple correlations among means are summarized in Table S4. The total zooplankton abundance showed negative correlations with all other parameters, recording maximum strength of association with Chl *a*, but the values were not statistically significant. Zooplankton taxon-specific correlation with Chl *a* gives insight, explaining the group-wise differential relationship: Rotifera ($R = -0.67$; $p < 0.01$) and Cladocera ($R = -0.43$; $p < 0.05$) showed a significant negative correlation with Chl *a*, whereas Copepoda ($R = -0.4$; $p < 0.1$) did not correlate significantly with Chl *a*. Among freshwater stations, Cladocera and Copepoda exhibited significant positive correlations in all the three sampling cruises. Rotifera concentration correlated negatively with bacterial concentration, pH, EC, salinity, nitrate, phosphate, and Ca^{++} levels (Table S6). Among biotic components, Chl *a* values were in a core position, showing negative correlation separately with all the three zooplankton groups, whereas the bacterial concentration showed significant negative correlation with rotifer fraction of the zooplankton only (Table S6).

4. Discussion

The observed spatio-temporal variations in zooplankton, phytoplankton, and bacterio-plankton concentrations and the interrelationship among taxa and spatial occurrence of the most abundant culturable bacterial strains in the HRE along the salinity level ranging from 0.01 to 25 (PSU) unequivocally confirm the complex nature and dynamicity of the estuary. The local complexity and seaward gradient of nutrient concentrations, salinity, turbidity, and Chl *a* [7,41,83] have been demonstrated in various estuarine ecosystems globally. The strength of association between zooplankton (separately with Rotifera, Cladocera, and Copepoda) with bacteria and Chl *a* in the present study provide additional insights into relative role of bacterial and algal carbon in supporting zooplankton community in highly dynamic, tropical estuary such as the HRE.

4.1. Interrelationship among Taxa

At upper stations, the rotifer community, recording lower abundance with higher diversity, exhibited significant negative correlation with bacterial concentrations, albeit bacteria and rotifer showed an overlapping relationship with abiotic parameters (e.g., pH, EC, salinity, TDS, nitrate, phosphate, and Ca^{++}). Similar physical requirements though significant negative correlation between Bacteria and Rotifera reflect strong grazing pressure by Rotifera on prokaryotes. On the other hand, the negative correlations of Chl *a* concentration with total zooplankton abundance in general and separately with all the zooplankton groups in particular suggest that zooplankton placed major grazing pressure on the phytoplankton community in the whole HRE. The prokaryotic community is controlled by the smaller zooplankton, particularly Rotifera, at the upstream stations. The majority of rotifers are filter-feeding and nanophagous which substantially utilize smaller organisms of the microbial web (bacteria and nano-flagellates and -ciliates) and are able to thrive on bacteria in eutrophic waters [32,84]. Earlier studies have reported the key role of autotrophic protists in shaping the zooplankton community structure by forming the base of food chain in the estuarine ecosystem [85,86].

The observed gradient in taxonomic diversity of zooplankton along the river to the sea continuum has also been reported in other estuaries [1,41,87]. The differences between the bacterial community in freshwater and estuarine systems can be explained by the fact that

the freshwater microbial community are directly under grazing pressure by the smaller zooplankton such as Rotifera, whereas at and around the confluence, microbial abundance is mainly controlled by the grazing pressure from developing stages of larger zooplankton or trophic cascade effect, where bacterivorous flagellates are grazed by Copepoda [85,88,89]. In line with this, previous studies have related microbial growth rates with rotifer grazing effects [90–93]. It may be noted that omnivores are a major controlling factor in estuarine stations, and this higher abundance of omnivorous zooplankton in downstream saline stations offsets the trophic cascade effects, resulting in higher bacterial abundance. The weak association of copepods with Chl *a* indicate bottom-up functioning of trophic cascade in estuaries. Omnivore-driven dampening of trophic cascades has been reported in other estuaries also [89,94].

4.2. Ecological Drivers of Planktonic Community Structure

The dissimilarity between sites (β -diversity) may reflect two different ecological situations: (i) It could reflect the loss of species from one site compared to the other. In this situation, the species present at one site are nested inside a larger set of species present at the other site. Alternatively, the following site records none of the species recorded at preceding site. In the latter case, there is a complete turnover of species between the two sites. In the HRE, both events occur concurrently, and the Bray–Curtis index takes into account both the components of dissimilarity. Further, in a distance-based multivariate model, variability among 72 samples based on riverine and estuarine locations was consistent with the main drivers, with salinity itself explaining 39.6%, 40.9%, and 37.4% variability, respectively, for rotifers, bacteria, and Chl *a* concentration. The freshwater-seawater salinity range is not continuous but rather subdivided in distinct stages, which is generally manifested in planktonic abundance [95]. The extensively used salinity classification is the Venice system that is 0–0.5, 0.5–5, 5–18, 18–30, and 30–40 (PSU). Further, based on salinity-range data, ref. [96] explained five salinity zones including 0–4, 2–14, 11–18, 16–27, and 24-marine. The present results based on explicit criteria of planktonic abundance along with the salinity range support the salinity classification by [96].

Surface water temperature increased downward from 26 to 29 °C with the average temperature value of 27.3 °C and showed significant positive correlation with bacteria and Chl *a* concentration. The role of temperature in maintaining planktonic community and invasion of alien species in estuary has been emphasized earlier [95]. Nutrient-related parameters (nitrate and phosphate) and TDS explain the higher abundance of Rotifera in upstream stations, where 56% of the factors determining Chl *a* concentration is the nitrate level and 52% of the factors contributing higher bacterial concentration is explained by the phosphate levels in the surface water. These microbes can use nitrate reductase, nitrite reductase, glutamine synthetase, and other compounds for nitrogen assimilation [97,98].

Ionic concentrations also show a vital role in unravelling the zooplankton, phytoplankton, and bacterioplankton community structure [99–101]. Hence, the discernible spatial distribution of most abundant bacterial strains and higher bacterial concentration at downstream stations can be explained by differential sodium and calcium requirements in bacterioplankton and phytoplankton. Freshwater and halophilic bacteria have overlapping physiological attributes but different sodium requirements. The marine strains require higher sodium and calcium level to grow, while freshwater and terrestrial strains such as *E. coli* can multiply at a higher rate without sodium [102]. In an estuary, the riverine and marine bacterial species, having ecologically similar physiological abilities but different sodium requirements, favor the halophilic strains (e.g., *Exiguobacterium aurantiacum* in present study) when freshwater from rivers enter the sea, as the sodium and calcium dependence does not constitute a fundamental ecological difference; rather, it only regulates the locally adapted strains responsible for them [42].

4.3. Spatio-Temporal Pattern

The lowermost riverine station is KDM, which grouped with upper freshwater stations during June 2018 and, in contrast, grouped together with lower estuarine stations during February 2018 (Figure 6). On the other hand, the clustering of June samples of upper two estuarine stations with freshwater stations is suggestive of a monsoon-based regime shift in the Hooghly estuary. A higher volume of freshwater discharge owing to pre-monsoon rainfall results in seaward extension of riverine biota, whereas in the case of lower discharge and reduced river flow during February, it leads to upward extension of marine biota into a lower freshwater station (KDM). The association of October samples of the KDM station was with the estuarine stations and February and June samples with upstream freshwater stations. This gives an insight in the seawater intrusion process in the HRE. This differential grouping of lower freshwater station with saline stations and with freshwater stations depending upon the season highlights the importance of stratification based on salinity in the suppression of turbulent vertical mixing in the estuary. In February and June, weak stratification and strong vertical mixing prevails during this period, and the riverine discharge counters the seawater intrusion. During the monsoon, the strength of the estuary circulation increases as river discharge rises, while the length of seawater intrusion diminishes. However, in October, during post-monsoon season, the suppression of turbulent mixing and the strength of the estuarine circulation is mostly determined by tidal velocity. Seawater incursion associated with estuary circulation reduces as tidal velocity rises but increases when river discharge rises [103]. In fact, Monsoon flows affect all facets of estuarine hydrobiology and community structure. In the light of monsoonal influence, the HRE may be called a “tropical monsoonal estuary” [104]. The monsoonal precipitation-driven rapid decline of salinity and surface runoffs limits the distribution of marine forms, whereas the intermediate condition favors rapid multiplication of the brackish water forms and re-assembly of the halotolerant groups, thereby resulting in the shifting regimes of transitional stations. This explains the seasonal shifting of the KDM station from freshwater to salt water, as observed in the present study. Other studies have shown the relevance of inshore water zones as zooplankton sources in large rivers such as the Danube [105,106] and St. Lawrence rivers [107]. Estuarine ecosystems in India show two peak periods, and peak time varies from region to region [108]. The present observation corroborates the previous results, in which two peaks were recorded in different months [18,109,110]. The spatial attributes of rivers are not always continuous [111], as proposed by [112]. Local land-driven discharge, changes in drought and flood regimes, and the establishment of diverse hydrological retention zones [113,114] (due to silt deposition) alter flow and river beds differentially during dry and wet seasons [113,115,116]. Therefore, results suggest that the phytoplankton, zooplankton, and bacterioplankton dynamics in the HRE are controlled by the interplay of hydrological regime, nutrient concentrations, and allochthonous inputs.

4.4. Spatial Occurrence of Highly Abundant Bacterial Strains

Bacterial study includes culture-based evaluation because studying morphology, ecology, bioprospecting for human use, and bioremediation for the purpose of culture-based isolation is practiced globally [117]. Consequently, while many environmental studies focus on large descriptions of microbial diversity through whole genome sequencing (WGS) approaches, other environmental studies rely on culturing approaches to estimate the abundance of a given culturable taxa in the environment. Both approaches are usually performed independently, and this does not allow direct comparison of the benefits and constraints of both methods. However, the culture-based approaches select only a subset of culturable bacteria, and it remains unclear to what extent culture-driven enrichments could be compared between different environmental samples. The present study depends on culture-based analysis, in which the upstream stations BRK and DKS recorded *Bacillus subtilis* and *Pseudomonas songnenensis* strains, and the lowermost station GS recorded *Exiguobacterium aurantiacum* as the highly abundant bacterial strain. The presence of soil

bacteria in upstream stations indicate the influence of land driven allochthonous discharge as the major contributory factor of bacterial abundance, which enters the aquatic food chain by the microbial degradation and remineralization and its recycling within the pelagic food web. Bacteria are the only organisms capable of recycling DOM, making them an essential component of ecosystem functioning [85]. The differences in bacterial populations could be due in part to differences we observed in DOM and DOC quantity and quality among the three samples, as it has previously been shown that DOM and DOC strongly structure bacterial communities in aquatic environments [118–120].

The differences in bacterial abundance can also be attributed to differential abundance and community composition of zooplankton, as they utilize bacteria directly or indirectly through many other bacterivorous organisms and establish the link to the traditional aquatic food web [121]. Consequently, ecological productivity in estuaries is affected by both top-down and bottom-up mechanisms. Top-down controls, such as meso-zooplankton grazing, may decrease micro-zooplankton populations, enabling phytoplankton species to bloom and altering the overall structure of the microbial community [87,121–123]. At riverine sites around Kolkata city, strong top-down effects are major regulators of bacterioplankton abundance by bacterivorous organisms [124]. Additionally, the lower rotifer abundance during the peak of copepod abundance at upstream freshwater stations is also suggestive of top-down control of rotifers by copepods [41,67,125,126]. In contrast, the dominance of omnivorous and herbivorous fractions of zooplankton and higher Chl *a* and bacterial concentrations near the estuary mouth reflect strong bottom-up impacts, where the nutrient-loaded environment favors microbial and phytoplankton growth that supports omnivorous species and all the trophic guilds in the absence of a distinct trophic cascade [89,93,127].

The bacterial abundance and physicochemical parameters, particularly nutrient concentrations and differential abundance of rotifers and cladocerans, are indicative of land-driven allochthonous influence from urban discharge of the metropolis city of Kolkata. The highest Chl *a* and Na⁺ at KCB preceding the confluence (GS) attest to the established facts that estuaries, particularly the mixing zone, are the most productive ecosystem and constitute an important system that provides valuable nursery and recruitment ground for commercially important species. However, with the development of sequencing technologies, further study is needed to elucidate the potential novel functions and phylogenetic relationships by sequencing the genomes of entire communities to understand relative contribution of bacterial community in HRE.

The instant change in community structure recorded in this study at lower salinity levels suggests the potential for underlying change in the oligohaline or limnetic stretches. In line with successful management of the San Francisco estuary based on isohaline condition [128], the present results indicate management options for the HRE, recommended as limited withdrawals to fixed fraction of total river flow beyond a minimum flow threshold [129]. The concerned administration needs to fix a minimum flow target in accordance with ideal region-specific isohalines in the estuary.

5. Conclusions

The zooplankton, phytoplankton, bacterioplankton, and abiotic parameters reported in this paper elucidate the patterns and drivers of differential community structures across the salinity gradient in the HRE. Among zooplankton, rotifers and cladocerans are numerically dominant and exert strong selection pressure on bacterial community and clear the suspended particles from the water column at upstream stations, whereas copepods play a major role in structuring microbial community at downstream estuarine stations. The negative correlation between Chl *a* and bacterial abundance, though insignificant, points to the competition for inorganic nutrients between phytoplankton and bacteria. Spatial variations in the trophic-based zooplankton community structure also suggest differential effects of direct bacterivore behavior by rotifers and omnivore-driven, suppressed trophic cascade effects through copepods, both of which concurrently play an important role in shaping the HRE community. The abiotic parameters such

as surface water temperature; elemental concentrations of Ca^{++} , Na^+ , and K^+ ; and the trophic level-related parameters (nitrate and phosphate) record significant seaward increase, which in turn reflects the increased concentrations of bacteria and Chl *a* (primary production) at downstream estuarine stations.

The three isolated strains of the most culturable bacteria at Barackpore, Dakshineswar, and Gangasagar, characterized as *Bacillus subtilis*, *Pseudomonas songnenensis*, and *Exiguobacterium aurantiacum*, indicate differential influences of land-driven discharge and spatial heterogeneity in the prokaryotic community structure. The observed alteration in planktonic community structure in the sampled stretch of the HRE points to larger impacts of water extraction and sewage discharge on salinity level, resulting in changes in the riverine community in the sampled limnetic-to-oligohaline stretches.

At the temporal scale, the increased river discharge during pre-monsoon and monsoon season plays an important role in shaping the community structure by upward extension of marine influence during the waning season but downward extension of river influence during the monsoon. Therefore, the complexity of phytoplankton, mesozooplankton, and prokaryote communities responding to variable elemental and nutrient concentrations is driven by the differential mixing of freshwater and marine sources. Both bottom-up and top-down effects play a vital role in shaping the community in the HRE.

Increased urbanization with uncontrolled water extraction, discharge of industrial and domestic wastes in coastal waters near the mouth of the Hooghly River, and shoreline development affect the planktonic community, consequentially affecting overall ecosystem health.

Furthermore, this study also highlights the role of land discharge at freshwater stations, season-specific seawater intrusion in the river, and abiotic variables including trophic status as drivers of abundance of the prokaryotic and eukaryotic planktonic community. These results suggest limited wastewater discharge and water withdrawals to a fixed fraction of total river flow beyond a minimum flow threshold maintaining isohaline. The concerned administration needs to fix a minimum flow target in accordance with ideal region-specific isohalines in the estuary. Therefore, for any future planning, the volume of water withdrawals and wastewater discharge, monsoon-driven regime shift, and internal trophic-based regulation mechanisms need to be considered.

Supplementary Materials: The following are available online at <https://www.mdpi.com/article/10.3390/jmse11010088/s1>, Figure S1: 1.2% Agarose gel showing single 1500 bp of 16S rDNA amplicon. Lane 1: 100bp DNA ladder; Lane 2: 16S rDNA amplicon of (A) BRK2, (B) DKS, and (C) GS1 strains. Table S1: Consensus sequence of the three strains BRK2, DKS, and GS1 characterized and their National Center for Biotechnology Information (NCBI) accession numbers and origin. Table S2: Physiochemical and biological parameters at six selected stations (BRK, DK2S, KDM, KDP, KCB, GS) in Hooghly River estuary. Table S3: Phytoplankton species recorded at six selected sampling stations in HRE during October 2017, February 2018, and June 2018. Table S4: Zooplankton taxa recorded at six selected sampling stations in HRE during October 2017, February 2018, and June 2018. Table S5: Zooplankton species/group identified for the present study, propensity of their feeding, and relevant references. Table S6: Pairwise Pearson correlation matrix between total zooplankton and major groups (Rotifera, Copepoda, Cladocera), with biotic (bacterial density, Chl *a*) and abiotic parameters (pH, EC, temperature, salinity, DO, total hardness, nitrate, phosphate, potassium, sodium, and calcium).

Author Contributions: R.K. conceived the concept; D.P. performed the field sampling data analyses; R.K. worked for interpretation of results and C.B.T. critically provided feedback and edited the manuscript. Both authors approved the submission of the manuscript. All authors have read and agreed to the published version of the manuscript.

Funding: Financial support was provided by the Department of Biotechnology, Government of India under river cleaning project (BT/PR20543/BCE/8/1398/2016).

Institutional Review Board Statement: Not applicable.

Informed Consent Statement: Not applicable.

Data Availability Statement: Data are available as Supplementary Materials. Additional data can be obtained on request to dprakashevs@cub.ac.in.

Acknowledgments: We are thankful to Department of Biotechnology for the project ((BT/PR20543/BCE/8/1398/2016)) to R.K. under the river-cleaning programme. D.P. thanks UGC for a National Fellowship.

Conflicts of Interest: The authors declare no conflict of interest.

References

1. Elliott, M.; McLusky, D.S. The need for definitions in understanding estuaries. *Estuar. Coast. Shelf Sci.* **2002**, *55*, 815–827. [[CrossRef](#)]
2. McLusky, D.S.; Elliott, M. Transitional waters: A new approach, semantics or just muddying the waters? *Estuar. Coast. Shelf Sci.* **2007**, *71*, 359–363. [[CrossRef](#)]
3. Whitfield, A.K.; Elliott, M. Fishes as indicators of environmental and ecological changes within estuaries: A review of progress and some suggestions for the future. *J. Fish Biol.* **2002**, *61*, 229–250. [[CrossRef](#)]
4. Chicharo, L.; Chicharo, M.A.; Ben-Hamadou, R. Use of a hydrotechnical infrastructure (Alqueva Dam) to regulate planktonic assemblages in the Guadiana estuary: Basis for sustainable water and ecosystem services management. *Estuar. Coast. Shelf Sci.* **2006**, *70*, 3–18. [[CrossRef](#)]
5. Tweedley, J.R.; Dittmann, S.R.; Whitfield, A.K.; Withers, K.; Hoeksema, S.D.; Potter, I.C. Hypersalinity: Global distribution, causes, and present and future effects on the biota of estuaries and lagoons. In *Coasts Estuaries*; Elsevier: Amsterdam, The Netherlands, 2019; Chapter 30; pp. 523–546. ISBN 9780128140031. [[CrossRef](#)]
6. Svetlichny, L.; Hubareva, E.; Khanaychenko, A.; Uttieri, M. Response to salinity and temperature changes in the alien Asian copepod *Pseudodiaptomus marinus* introduced in the Black Sea. *J. Exp. Zool.* **2019**, *331*, 416–426. [[CrossRef](#)] [[PubMed](#)]
7. Cloern, J.E.; Jassby, A.D. Patterns and scales of phytoplankton variability in estuarine–coastal ecosystems. *Estuaries Coasts* **2010**, *33*, 230–241. [[CrossRef](#)]
8. Cloern, J.E.; Foster, S.Q.; Kleckner, A.E. Phytoplankton primary production in the world’s estuarine–coastal ecosystems. *Biogeo-science* **2014**, *11*, 2477–2501. [[CrossRef](#)]
9. Cloern, J.E.; Jassby, A.D.; Schraga, T.S.; Nejad, E.; Martin, C. Ecosystem variability along the estuarine salinity gradient: Examples from long-term study of San Francisco Bay. *Limnol. Oceanogr.* **2017**, *62*, S272–S291. [[CrossRef](#)]
10. Testa, J.M.; Murphy, R.R.; Brady, D.C.; Kemp, W.M. Nutrient-and climate-induced shifts in the phenology of linked biogeochemical cycles in a temperate estuary. *Front. Mar. Sci.* **2018**, *5*, 114. [[CrossRef](#)]
11. Hume, T.M.; Snelder, T.; Weatherhead, M.; Liefing, R. A controlling factor approach to estuary classification. *Ocean Coast. Manag.* **2007**, *50*, 905–929. [[CrossRef](#)]
12. Dürr, H.H.; Laruelle, G.G.; van Kempen, C.M.; Slomp, C.P.; Meybeck, M.; Middelkoop, H. Worldwide typology of nearshore coastal systems: Defining the estuarine filter of river inputs to the oceans. *Estuaries Coasts* **2011**, *34*, 441–458. [[CrossRef](#)]
13. Chilton, D.; Hamilton, D.P.; Nagelkerken, I.; Cook, P.; Hipsey, M.R.; Reid, R.; Sheaves, M.; Waltham, N.J.; Brookes, J. Environmental Flow Requirements of Estuaries: Providing Resilience to Current and Future Climate and Direct Anthropogenic Changes. *Front. Environ. Sci.* **2021**, *9*, 764218. [[CrossRef](#)]
14. Azam, F.; Fenchel, T.; Field, J.G.; Gray, J.S.; Meyer-Reil, L.A.; Thingstad, F. The ecological role of water-column microbes in the sea. *Mari. Ecol. Prog. Serie.* **1983**, *10*, 257–263. [[CrossRef](#)]
15. Mikhailov, I.S.; Zakharova, Y.R.; Bukin, Y.S.; Galachyants, Y.P.; Petrova, D.P.; Sakirko, M.V.; Likhoshway, Y.V. Co-occurrence networks among bacteria and microbial eukaryotes of Lake Baikal during a spring phytoplankton bloom. *Mic. Eco.* **2019**, *77*, 96–109. [[CrossRef](#)]
16. Yang, Y.; Gao, Y.; Chen, Y.; Li, S.; Zhan, A. Interaction-based abiotic and biotic impacts on biodiversity of plankton communities in disturbed wetlands. *Div. Dist.* **2019**, *25*, 1416–1428. [[CrossRef](#)]
17. Roy, A.P.; Pandit, A.R.; Sharma, A.P.; Bhaumik, U.T.; Majunder, S.; Biswas, D.K. Socioeconomic status and livelihood of fisher women of Hooghly estuary. *Inland Fish. Soc. India* **2015**, *47*, 49–56.
18. Dutta, N.; Malhotra, J.C.; Bose, B.B. Hydrology and seasonal fluctuations of the plankton in the Hooghly estuary. In *Symposium on Marine and Freshwater Plankton in the Indo-Pacific*; Indo-Pacific Fisheries Council: Bangkok, Thailand, 1954; pp. 35–47.
19. Bose, B.B. Observations on the hydrology of the Hooghly Estuary. *Inland J. Fish.* **1956**, *3*, 101–118.
20. Manna, R.K.; Satpathy, B.B.; Roshith, C.M.; Naskar, M.; Bhaumik, U.; Sharma, A.P. Spatio-temporal changes of hydro-chemical parameters in the estuarine part of the river Ganges under altered hydrological regime and its impact on biotic communities. *Aquat. Ecosyst. Health Manag.* **2013**, *16*, 433–444. [[CrossRef](#)]
21. Das, B.K.; Ray, A.; Johnson, C.; Verma, S.K.; Alam, A.; Baitha, R.; Sarkar, U.K. The present status of ichthyofaunal diversity of river Ganga India: Synthesis of present v/s past. *Acta Ecol. Sin.* **2021**, in press. [[CrossRef](#)]
22. Ramesh, R.; Lakshmi, A.; Sappal, S.M.; Bonthu, S.R.; Suganya, M.D.; Ganguly, D.; Purvaja, R. Integrated management of the Ganges delta, India. *Coas. Estu.* **2019**, 187–211. [[CrossRef](#)]
23. ICAR—Central Inland Fisheries Research Institute. *Assessment of Fish and Fisheries of the Ganga River System for Developing Suitable Conservation and Restoration Plan*; Sanctioned under National Mission on Clean Ganga, vide NGRBA Order NO.T-17 /2014 15/526/NMCG-Fish and Fisheries Dated 13 July 2015; CFRI: Barrackpore, India, 2019.

24. Bhaumik, U.; Sharma, A.P. The fishery of Indian Shad (*Tenulosa ilisha*) in the Bhagirathi-Hooghly river system. *Fish. Chimes* **2011**, *31*, 21–27.
25. Sharma, A.P.; Joshi, K.D.; Naskar, M.; Das, M.K. *Inland Fisheries & Climate Change: Vulnerability and Adaptation Options*; NICRA: Phek, India, 2014.
26. Bianchi, F.; Aciri, F.; Aubry, F.B.; Berton, A.; Boldrin, A.; Camatti, E.; Cassin, D.; Comaschi, A. Can plankton communities be considered as bioindicators of water quality in the lagoon of Venice? *Mar. Pollut. Bull.* **2003**, *46*, 964–971. [[CrossRef](#)] [[PubMed](#)]
27. Hsiao, S.H.; Lee, C.Y.; Shih, C.T.; Hwang, J.S. Calanoid copepods of the Kuroshio Current east of Taiwan, with a note on the presence of *Calanus jashnovi* Hulseman, 1994. *Zool. Stud.* **2004**, *43*, 323–331.
28. Pomeroy, L.R.; Leb, W.P.J.; Azam, F.; Hobbie, J.E. The microbial loop. *Oceanography* **2007**, *20*, 28–33. [[CrossRef](#)]
29. Orellana, M.V.; Pang, W.L.; Durand, P.M.; Whitehead, K.; Baliga, N.S. A role for programmed cell death in the microbial loop. *PLoS ONE* **2013**, *8*, e62595. [[CrossRef](#)]
30. Degerman, R.; Lefébure, R.; Byström, P.; Båmstedt, U.; Larsson, S.; Andersson, A. Food web interactions determine energy transfer efficiency and top consumer responses to inputs of dissolved organic carbon. *Hydrobiologia* **2018**, *805*, 131–146. [[CrossRef](#)]
31. Fenchel, T. The microbial loop—25 years later. *J. Exp. Mar. Bio. Ecol.* **2008**, *366*, 99–103. [[CrossRef](#)]
32. Prakash, D.; Kumar, R.; Rajan, K.; Patel, A.; Yadav, D.; Dhankar, R.; Khudssar, A.F. Integrated application of macrophytes and zooplankton for wastewater treatment. *Front. Environ. Sci. Water Wastewater Manag.* **2022**, *10*, 941841. [[CrossRef](#)]
33. Bachy, C.; Hehenberger, E.; Ling, Y.C.; Needham, D.M.; Strauss, J.; Wilken, S.; Worden, A.Z. Marine Protists: A Hitchhiker’s Guide to their Role in the Marine Microbiome. In *The Marine Microbiome*; Springer: Cham, Switzerland, 2022; pp. 159–241. [[CrossRef](#)]
34. Kumar, R. Feeding modes and associated mechanisms in Zooplankton. In *Ecology of Plankton*; Kumar, A., Ed.; Daya Publishing House: Delhi, India, 2004; pp. 220–226.
35. Kumar, R.; Rao, T.R. Demographic responses of adult *Mesocyclops thermocyclopoides* (Copepoda, Cyclopoida) to different plant and animal diets. *Freshw. Biol.* **1999**, *42*, 487–501. [[CrossRef](#)]
36. Roy, S.P.; Roy, R.; Prabhakar, A.K.; Pandey, A.; Kumar, R.; Tseng, L.C. Spatio-temporal distribution and community structure of zooplankton in the Gangetic Dolphin Sanctuary, 2009. *Aquat. Ecosyst. Health Manag.* **2013**, *16*, 374–384. [[CrossRef](#)]
37. Sarkar, S.K.; Singh, B.N.; Choudhury, A. The ecology of copepods from Hoogly estuary, west Bengal, India. *Mahasagar-Bull. Natl. Inst. Oceanogr.* **1986**, *19*, 103–112.
38. Roshith, C.M.; Meena, D.K.; Manna, R.K.; Sahoo, A.K.; Swain, H.S.; Raman, R.K.; Das, B.K. Phytoplankton community structure of the Gangetic (Hooghly-Matla) estuary: Status and ecological implications in relation to eco-climatic variability. *Flora* **2018**, *240*, 133–143. [[CrossRef](#)]
39. Waniek, J.J. The role of physical forcing in initiation of spring blooms in the northeast Atlantic. *J. Mar. Syst.* **2003**, *39*, 57–82. [[CrossRef](#)]
40. Sridhar, R.; Thangaradjou, T.; Senthil, K.S.; Kannan, L. Water quality and phytoplankton characteristics in the Palk Bay, southeast coast of India. *J. Environ. Biol.* **2006**, *27*, 561–566.
41. Hwang, J.S.; Kumar, R.; Hsieh, C.W.; Kuo, A.Y.; Souissi, S.; Hsu, M.H.; Chen, Q.C. Patterns of zooplankton distribution along the marine, estuarine and riverine portions of the Danshuei ecosystem in northern Taiwan. *Zool. Stud.* **2010**, *49*, 335–352.
42. Wang, Q.; Hao, Z.; Ding, R.; Li, H.; Tang, X.; Chen, F. Host dependence of zooplankton-associated microbes and their ecological implications in freshwater lakes. *Water* **2021**, *13*, 2949. [[CrossRef](#)]
43. Ling, L.L.; Schneider, T.; Peoples, A.J.; Spoering, A.L.; Engels, I.; Conlon, B.P.; Lewis, K. A new antibiotic kills pathogens without detectable resistance. *Nature* **2015**, *517*, 455–459. [[CrossRef](#)]
44. Sarkar, S.K.; Saha, M.; Takada, H.; Bhattacharya, A.; Mishra, P.; Bhattacharya, B. Water quality management in the lower stretch of the river Ganges, east coast of India: An approach through environmental education. *J. Clean. Prod.* **2007**, *15*, 1559–1567. [[CrossRef](#)]
45. Beyrend-Dur, D.; Kumar, R.; Rao, T.R.; Souissi, S.; Cheng, S.H.; Hwang, J.S. Demographic parameters of adults of *Pseudodiaptomus annandalei* (Copepoda: Calanoida): Temperature–salinity and generation effects. *J. Exp. Mari. Biol. Ecol.* **2011**, *404*, 1–14. [[CrossRef](#)]
46. Strickland, J.D.H.; Parsons, T.R. *A Practical Handbook of Seawater Analysis*; Fisheries Research Board of Canada: Ottawa, ON, Canada, 1972.
47. APHA. *Standard Methods for the Examination of Water and Wastewater*, 21st ed.; American Public Health Association (APHA): Washington, DC, USA, 2005.
48. Aneja, K.R. *Experiments in Microbiology, Plant Pathology and Biotechnology*; NewAge International: Lincolnshire, UK, 2007; p. 58.
49. Selvin, J.; Lanong, S.; Syiem, D.; De Mandal, S.; Kayang, H.; Kumar, N.S.; Kiran, G.S. Culture-dependent and metagenomic analysis of lesser horseshoe bats’ gut microbiome revealing unique bacterial diversity and signatures of potential human pathogens. *Micr. Patho.* **2019**, *137*, 103675. [[CrossRef](#)] [[PubMed](#)]
50. Böttger, E.C. Rapid determination of bacterial ribosomal RNA sequences by direct sequencing of enzymatically amplified DNA. *FEMS Microbiol. Lett.* **1989**, *65*, 171–176. [[CrossRef](#)]
51. Tamura, K.; Nei, M. Estimation of the number of nucleotide substitutions in the control region of mitochondrial DNA in humans and chimpanzees. *Mol. Bio. Evol.* **1993**, *10*, 512–526. [[CrossRef](#)]
52. Tamura, K.; Stecher, G.; Kumar, S. MEGA11, molecular evolutionary genetics analysis version 11. *Mol. Bio. Evol.* **2021**, *38*, 3022–3027. [[CrossRef](#)] [[PubMed](#)]

53. John, D.M.; Whitton, B.A.; Brook, A.J. *The Freshwater Algal flora of the British Isles: An Identification Guide to Freshwater and Terrestrial Algae*; Cambridge University Press: Cambridge, UK, 2002.
54. Prescott, G.W. *How to Know the Fresh-Water Algae—An Illustrated Key for the Identifying the More Common Freshwater Algae to Genus, with Hundreds of Species Named and Pictured and with Numerous Aids for the Study*; W.C. Brown Co.: Dubuque, IA, USA, 1964; p. 293.
55. Singh, J.; Saxena, R.C. An Introduction to Microalgae: Diversity and Significance. In *Handbook of Marine Microalgae*; Academic Press: Cambridge, MA, USA, 2015; pp. 11–24. [CrossRef]
56. Guiry, M.D.; Guiry, G.M. *Algae Base*. World-Wide Electronic Publication, National University of Ireland, Galway. 2022. Available online: <http://www.algaebase.org/> (accessed on 12 July 2018).
57. Singh, P.; Gupta, S.K.; Guldhe, A.; Rawat, I.; Bux, F. Microalgae Isolation and Basic Culturing Techniques. In *Handbook of Marine Microalgae*; Elsevier Inc.: Amsterdam, The Netherlands, 2015; pp. 43–54. [CrossRef]
58. Shoaf, W.T.; Lium, B.W. Improved extraction of Chlorophyll *a* and *b* from algae using dimethyl sulfoxide. *Limnol. Oceanogr.* **1976**, *21*, 926–928. [CrossRef]
59. Parsons, T.R.; Maita, Y.; Lalli, C.M. *A Manual of Chemical and Biological Methods for Seawater Analysis*; Pergamon Press: Oxford, UK, 1984; p. 173.
60. Sehgal, K.L. *Planktonic Copepods of Freshwater Ecosystems*; Inter Print: New Delhi, India, 1983.
61. Michael, R.G.; Sharma, B.K. *Indian Cladocera (Crustacea, Branchiopoda, Cladocera)*; Zoological Survey of India: Kolkata, India, 1988; p. 262.
62. Dodson, S.I.; Frey, D.G. Cladocera and other branchiopoda. In *Ecology and Classification of North American Freshwater Invertebrates*; Thorp, J.H., Covich, A.P., Eds.; Academic Press: New York, NY, USA, 1991; pp. 764–776.
63. Edmondson, W.T. *Fresh-Water Biology, Wipple and Ward Reprint (Indian Reprint)*; International Books & Periodicals Supply Service: New Delhi, India, 1992; p. 24B/5.
64. Battish, S.K. *Freshwater Zooplankton of India*; Oxford and IBH Publishing Co., Pvt., Ltd.: New Delhi, India, 1992.
65. Sharma, B.K. *Freshwater Rotifers (Rotifers: Eurotatoria) Fauna of West Bengal State Faunal Series*; Zoological Survey of India: Calcutta, India, 1992; Volume 3, pp. 1–121.
66. Dumont, H.J. On the diversity of Cladocera in the tropics. *Hydrobiologia* **1994**, *272*, 27–38. [CrossRef]
67. Kumar, R. Effect of *Mesocyclops thermocyclopoides* (Copepoda, Cyclopoida) predation on population dynamics of different prey: A laboratory study. *J. Freshw. Ecol.* **2003**, *18*, 383–393. [CrossRef]
68. Ramakrishna Rao, T.; Kumar, R. Patterns of prey selectivity in the cyclopoid copepod *Mesocyclops thermocyclopoides*. *Aqua. Ecol.* **2002**, *36*, 411–424. [CrossRef]
69. Fernando, C.H. *A Guide to Tropical Freshwater Zooplankton, Identification, Ecology and Impact on Fisheries*; Backhuys Publishers: Leiden, The Netherlands, 2002.
70. Tseng, L.C.; Kumar, R.; Dahms, H.U.; Chen, Q.C.; Hwang, J.S. Monsoon-driven succession of copepod assemblages in coastal waters of the northeastern Taiwan Strait. *Zool. Stud.* **2008**, *47*, 46.
71. Kumar, R.; Souissi, S.; Hwang, J.S. Vulnerability of carp larvae to copepod predation as a function of larval age and body length. *Aquaculture* **2012**, *338*, 274–283. [CrossRef]
72. Voigt, M.; Koste, W. *Rotatoria, Die Rädertiere Mitteleuropas*, 2nd ed.; Gebrüder Borntraeger: Stuttgart, Germany, 1978; Volume 1, 673p.
73. Brandl, Z. Freshwater copepods and rotifers: Predators and their prey. In *Rotifera X*; Springer: Dordrecht, NJ, USA, 2005; pp. 475–489. [CrossRef]
74. Ooms-Wilms, A.L.; Postema, G.; Gulati, R.D. Evaluation of bacterivory of Rotifera based on measurements of in situ ingestion of fluorescent particles, including some comparisons with Cladocera. *J. Plank. Resea.* **1995**, *17*, 1057–1077. [CrossRef]
75. Starkweather, P.L.; Gilbert, J.J.; Frost, T.M. Bacterial feeding by the rotifer *Brachionus calyciflorus*: Clearance and ingestion rates, behavior and population dynamics. *Oecologia* **1979**, *44*, 26–30. [CrossRef] [PubMed]
76. Kim, H.W.; Hwang, S.J.; Joo, G.J. Zooplankton grazing on bacteria and phytoplankton in a regulated large river (Nakdong River, Korea). *J. Plank. Res.* **2000**, *22*, 1559–1577. [CrossRef]
77. Leasi, F.; Ricci, C. Musculature of two bdelloid rotifers, *Adineta ricciae* and *Macrotrachela quadricornifera*: Organization in a functional and evolutionary perspective. *J. Zool. Syst. Evol. Res.* **2010**, *48*, 33–39. [CrossRef]
78. Kiørboe, T. How zooplankton feed: Mechanisms, traits and trade-offs. *Bio. Rev.* **2011**, *86*, 311–339. [CrossRef]
79. Field, J.G.; Clarke, K.R.; Warwick, R.M. A practical strategy for analysing multispecies distribution patterns. *Mar. Ecol. Prog. Ser.* **1982**, *8*, 37–52. [CrossRef]
80. Pielou, E.C. The measurement of diversity in different types of biological collections. *J. Theor. Biol.* **1966**, *13*, 131–144. [CrossRef]
81. Margalef, R. Some concepts relative to the organization of plankton. *Oceanogr. Mar. Biol. Annu. Rev.* **1967**, *5*, 257–289.
82. Hunt, B.P.V.; Pakhomov, E.A.; Trotsenko, B.G. The macrozooplankton of the Cosmonaut Sea, east Antarctica (30° E–60° E), 1987–1990. *Deep-Sea Res. Pt. I Oceanogr.* **2007**, *54*, 1042–1069. [CrossRef]
83. Azhikodan, G.; Yokoyama, K. Spatio-temporal variability of phytoplankton (Chlorophyll-*a*) in relation to salinity, suspended sediment concentration, and light intensity in a macrotidal estuary. *Cont. Shelf Res.* **2016**, *126*, 15–26. [CrossRef]
84. Gilbert, J.J. Food niches of planktonic rotifers: Diversification and implications. *Limnol. Oceanogr.* **2022**, *67*, 2218–2251. [CrossRef]
85. Zöllner, E.; Hoppe, H.G.; Sommer, U.; Jürgens, K. Effect of zooplankton-mediated trophic cascades on marine microbial food web components (bacteria, nanoflagellates, ciliates). *Limnol. Oceanogr.* **2009**, *54*, 262–275. [CrossRef]

86. Dalu, T.; Froneman, P.W.; Richoux, N.B. Phytoplankton community diversity along a river-estuary continuum. *Trans. R. Soc. South Afr.* **2014**, *69*, 107–116. [[CrossRef](#)]
87. Murrell, M.C.; Stanley, R.S.; Loes, E.M.; Di Donato, G.T.; Flemer, D.A. Linkage between microzooplankton grazing and phytoplankton growth in a Gulf of Mexico estuary. *Estuaries* **2002**, *25*, 19–29. [[CrossRef](#)]
88. Hobbie, J.E. A comparison of the ecology of planktonic bacteria in fresh and salt water. *Limnol. Oceanogr.* **1988**, *33*, 750–764. [[CrossRef](#)]
89. Johnson, K.D.; Grabowski, J.; Smee, D.L. Omnivory dampens trophic cascades in estuarine communities. *Mari. Ecol. Prog. Seri.* **2014**, *507*, 197–206. [[CrossRef](#)]
90. McManus, G.B.; Ederington-Cantrell, M.C. Phytoplankton pigments and growth rates, and microzooplankton grazing in a large temperate estuary. *Mar. Eco. Prog. Ser.* **1992**, *87*, 77–85. [[CrossRef](#)]
91. Lehrter, J.C.; Pennock, J.R.; McManus, G.B. Microzooplankton grazing and nitrogen excretion across a surface estuarine-coastal interface. *Estuaries* **1999**, *22*, 113–125. [[CrossRef](#)]
92. Chen, G.Q. A microbial polyhydroxyalkanoates (PHA) based bio-and materials industry. *Che. Soc. Rev.* **2009**, *38*, 2434–2446. [[CrossRef](#)] [[PubMed](#)]
93. York, J.K.; McManus, G.B.; Kimmerer, W.J.; Slaughter, A.M.; Ignoffo, T.R. Trophic links in the plankton in the low salinity zone of a large temperate estuary: Top-down effects of introduced copepods. *Estuaries Coasts* **2014**, *37*, 576–588. [[CrossRef](#)]
94. Fahimipour, A.K.; Levin, D.A.; Anderson, K.E. Omnivory does not preclude strong trophic cascades. *Ecosphere* **2019**, *10*, e02800. [[CrossRef](#)]
95. Svetlichny, L.; Hubareva, E.; Uttieri, M. Ecophysiological and behavioural responses to salinity and temperature stress in cyclopoid copepod *Oithona davisae* with comments on gender differences. *Mediterr. Mar. Sci.* **2021**, *22*, 89–101. [[CrossRef](#)]
96. Bulger, A.J.; Hayden, B.P.; Monaco, M.E.; Nelson, D.M.; McCormick-Ray, M.G. Biologically-based estuarine salinity zones derived from a multivariate analysis. *Estuaries* **1993**, *16*, 311–322. [[CrossRef](#)]
97. Jetten, M.S.M. The microbial nitrogen cycle. *Environ. Microbiol.* **2008**, *10*, 2903–2909. [[CrossRef](#)]
98. Kanamori, K.; Weiss, R.L.; Roberts, J.D. Ammonia assimilation in *Bacillus polymyxa*. ¹⁵N NMR and enzymatic studies. *J. Biol. Chem.* **1987**, *262*, 11038–11045. [[CrossRef](#)]
99. Zhou, J.; Richlen, M.L.; Sehein, T.R.; Kulis, D.M.; Anderson, D.M.; Cai, Z. Microbial community structure and associations during a marine dinoflagellate bloom. *Front. Microbiol.* **2018**, *9*, 1201. [[CrossRef](#)]
100. Bickel, S.L.; Tang, K.W.; Grossart, H.P. Structure and function of zooplankton-associated bacterial communities in a temperate estuary change more with time than with zooplankton species. *Aquat. Microb. Ecol.* **2014**, *72*, 1–15. [[CrossRef](#)]
101. Lehman, P.W.; Kurobe, T.; Huynh, K.; Lesmeister, S.; Teh, S.J. Covariance of Phytoplankton, Bacteria, and Zooplankton Communities Within Microcystis Blooms in San Francisco Estuary. *Front. Microbiol.* **2021**, *12*, 1184. [[CrossRef](#)]
102. Hrenovic, J.; Ivankovic, T. Survival of *Escherichia coli* and *Acinetobacter junii* at various concentrations of sodium chloride. *EurAsian J. Biosci.* **2009**, *3*, 144–151. [[CrossRef](#)]
103. Bricheno, L.M.; Wolf, J.; Sun, Y. Saline intrusion in the Ganges-Brahmaputra-Meghna megadelta. *Estuar. Coast. Shelf Sci.* **2021**, *252*, 107246. [[CrossRef](#)]
104. Rath, A.R.; Mitbavkar, S.; Anil, A.C. Response of the phytoplankton community to seasonal and spatial environmental conditions in the Haldia port ecosystem located in the tropical Hooghly River estuary. *Environ. Monit. Assess.* **2021**, *193*, 1–24. [[CrossRef](#)] [[PubMed](#)]
105. Reckendorfer, W.; Keckeis, H.; Winkler, G.; Schiemer, F. Abundance in the River Danube, Austria: Ce of inshore retention. *Freshw. Biol.* **1999**, *41*, 583–591. [[CrossRef](#)]
106. Paul, S.; Karan, S.; Ghosh, S.; Bhattacharya, B.D. Hourly variation of environment and copepod community of the Ganges River Estuary of India: Perspectives on sampling estuarine zooplankton. *Estuar. Coast. Shelf Sci.* **2019**, *230*, 106441. [[CrossRef](#)]
107. Casper, A.F.; Thorp, J.H. Diel and lateral patterns of zooplankton distribution in the St. Lawrence River. *River Res. Appl.* **2007**, *23*, 73–85. [[CrossRef](#)]
108. Vijith, V.; Sundar, D.; Shetye, S.R. Time-dependence of salinity in monsoonal estuaries. *Estuar. Coast. Shelf Sci.* **2009**, *85*, 601–608. [[CrossRef](#)]
109. Shetty, H.P.C.; Saha, S.B.; Ghosh, B.B. Observations on the distribution and fluctuations of plankton in the Hooghly-Matlah estuarine system, with notes on their relation to commercial fish landings. *Indian J. Fish.* **1961**, *8*, 326–363.
110. Baidya, A.U.; Choudhury, A. Distribution and abundance of zooplankton in a tidal creek of Sagar Island, Sundarbans, West Bengal. *Environ. Ecol.* **1984**, *2*, 333–337.
111. Ward, J.W.; Stanford, J.A. *Intermediate-Disturbance Hypothesis: An Explanation for Biotic Diversity Patterns in Lotic Ecosystems; Dynamics of Lotic Systems*, Ann Arbor Science: Ann Arbor, MI, USA, 1983; pp. 347–356.
112. Vannote, R.L.; Minshall, G.W.; Cummins, K.W.; Sedell, J.R.; Cushing, C.E. The river continuum concept. *Can. J. Fish. Aquat. Sci.* **1980**, *37*, 130–137. [[CrossRef](#)]
113. Schiemer, F.; Keckeis, H.; Reckendorfer, W.; Winkler, G. The “inshore retention concept” and its significance for large rivers. *Arch. Hydrobiol.* **2001**, *135*, 509–516. [[CrossRef](#)]
114. Picapedra, P.H.; Fernandes, C.; Baumgartner, G.; Lansac-Tôha, F.A. Effect of slackwater areas on the establishment of plankton communities (testate amoebae and rotifers) in a large river in the semi-arid region of northeastern Brazil. *Limnetica* **2018**, *37*, 19–31. [[CrossRef](#)]

115. Medeiros, E.S.; Arthington, A.H. Allochthonous and autochthonous carbon sources for fish in floodplain lagoons of an Australian dryland river. *Environ. Biol. Fishes* **2011**, *90*, 1–17. [[CrossRef](#)]
116. Lucena, L.C.A.; Melo, T.X.D.; Medeiros, E.S.F. Zooplankton community of Parnaíba River, Northeastern Brazil. *Acta Limnol. Brasiliæ* **2015**, *27*, 118–129. [[CrossRef](#)]
117. Li, Y.; Wu, C.; Zhou, M.; Wang, E.T.; Zhang, Z.; Liu, W.; Xie, Z. Diversity of cultivable protease-producing bacteria in Laizhou Bay sediments, Bohai Sea, China. *Front. Microbiol.* **2017**, *8*, 405. [[CrossRef](#)] [[PubMed](#)]
118. Judd, K.E.; Crump, B.C.; Kling, G.W. Variation in dissolved organic matter controls bacterial production and community composition. *Ecology* **2006**, *87*, 2068–2079. [[CrossRef](#)] [[PubMed](#)]
119. Berge, O.; Monteil, C.L.; Bartoli, C.; Chandeysson, C.; Guilbaud, C.; Sands, D.C.; Morris, C.E. A user's guide to a data base of the diversity of *Pseudomonas syringae* and its application to classifying strains in this phylogenetic complex. *PLoS ONE* **2014**, *9*, e105547. [[CrossRef](#)]
120. Llíros, M.; Inceoğlu, Ö.; García-Armisen, T.; Anzil, A.; Leporcq, B.; Pigneur, L.-M.; Viroux, L.; Darchambeau, F.; Descy, J.-P.; Servais, P. Bacterial community composition in three freshwater reservoirs of different alkalinity and trophic status. *PLoS ONE* **2014**, *9*, e116145. [[CrossRef](#)]
121. Wollrab, S.; Diehl, S.; De Roos, A. MSimple rules describe bottom-up and top-down control in food webs with alternative energy pathways. *Ecol. Lett.* **2012**, *15*, 935–946. [[CrossRef](#)]
122. Buskey, E.J.; Montagna, P.A.; Amos, A.F.; Whitledge, T.E. Disruption of grazer populations as a contributing factor to the initiation of the Texas brown tide algal bloom. *Limnol. Oceanogr.* **1997**, *42*, 1215–1222. [[CrossRef](#)]
123. Ger, K.A.; Urrutia-Cordero, P.; Frost, P.C.; Hansson, L.A.; Sarnelle, O.; Wilson, A.E.; Lürling, M. The interaction between cyanobacteria and zooplankton in a more eutrophic world. *Harmful Algae* **2016**, *54*, 128–144. [[CrossRef](#)]
124. Yoshida, T.; Jones, L.E.; Ellner, S.P.; Fussmann, G.F.; Hairston, N.G. Rapid evolution drives ecological dynamics in a predator–prey system. *Nature* **2003**, *424*, 303–306. [[CrossRef](#)]
125. Kumar, R.; Rao, T.R. Effect of the cyclopoid copepod *Mesocyclops thermocyclopoides* on the interactions between the predatory rotifer *Asplanchna intermedia* and its prey *Brachionus calyciflorus* and *B. angularis*. *Hydrobiologia* **2001**, *453/454*, 261–268. [[CrossRef](#)]
126. Rosińska, J.; Romanowicz-Brzozowska, W.; Kozak, A.; Gołdyn, R. Zooplankton changes during bottom-up and top-down control due to sustainable restoration in a shallow urban lake. *Environ. Sci. Pollut. Res.* **2019**, *26*, 19575–19587. [[CrossRef](#)]
127. Glibert, P.M.; Fullerton, D.; Burkholder, J.M.; Cornwell, J.C.; Kana, T.M. Ecological stoichiometry, biogeochemical cycling, invasive species, and aquatic food webs: San Francisco Estuary and comparative systems. *Revie. Fish. Scie.* **2011**, *19*, 358–417. [[CrossRef](#)]
128. Kimmerer, W.J. Physical, biological, and management responses to variable freshwater flow into the San Francisco Estuary. *Estuaries* **2002**, *25*, 1275–1290. [[CrossRef](#)]
129. Flannery, M.S.; Peebles, E.B.; Montgomery, R.T. A percent-of-flow approach for managing reductions of freshwater inflows from unimpounded rivers to southwest Florida estuaries. *Estuaries* **2002**, *25*, 1318–1332. [[CrossRef](#)]

Disclaimer/Publisher's Note: The statements, opinions and data contained in all publications are solely those of the individual author(s) and contributor(s) and not of MDPI and/or the editor(s). MDPI and/or the editor(s) disclaim responsibility for any injury to people or property resulting from any ideas, methods, instructions or products referred to in the content.